Inorganic Chemistry

Article

pubs.acs.org/IC

Trivalent Uranium Phenylchalcogenide Complexes: Exploring the Bonding and Reactivity with CS_2 in the Tp^*_2UEPh Series (E = O, S, Se, Te)

Ellen M. Matson,[†] Andrew T. Breshears,[‡] John J. Kiernicki,[†] Brian S. Newell,[§] Phillip E. Fanwick,[†] Matthew P. Shores,[§] Justin R. Walensky,*[,‡] and Suzanne C. Bart*[,†]

[†]H.C. Brown Laboratory, Department of Chemistry, Purdue University, West Lafayette 47907, Indiana, United States

[‡]Department of Chemistry, University of Missouri, Columbia, Missouri 65211, United States

[§]Department of Chemistry, Colorado State University, Fort Collins, Colorado 80523, United States

Supporting Information

ABSTRACT: The trivalent uranium phenylchalcogenide series, Tp^*_2UEPh (Tp^* = hydrotris(3,5-dimethylpyrazolyl)borate, E = O (**1**), S (**2**), Se (**3**), Te (**4**)), has been synthesized to investigate the nature of the U−E bond. All compounds have been characterized by ^1H NMR, infrared and electronic absorption spectroscopies, and in the case of **4**, X-ray crystallography. Compound **4** was also studied by SQUID magnetometry. Computational studies establish Mulliken spin densities for the uranium centers ranging from 3.005 to 3.027 (B3LYP), consistent for uranium−chalcogenide bonds that are primarily ionic in nature, with a small covalent contribution. The reactivity of **2**−**4** toward carbon disulfide was also investigated and showed reversible CS_2 insertion into the U(III)−E bond, forming $Tp^*_2U(\kappa^2\text{-}S_2CEPh)$ (E = S (**5**), Se (**6**), Te (**7**)). Compound **5** was characterized crystallographically.

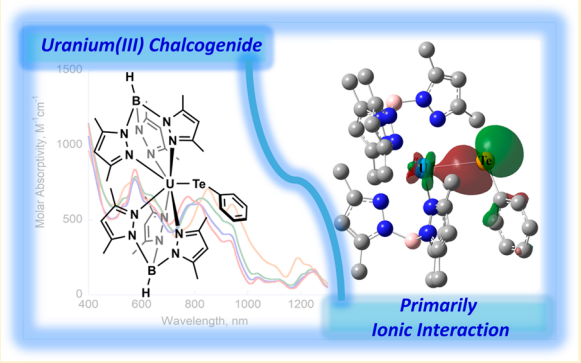

INTRODUCTION

For nuclear energy to be viable as an efficient energy source, the nuclear fuel cycle must be completed by recycling of the complicated mixture of heavy elements in the spent fuel.[1] Understanding uranium−ligand bonding to find distinguishing characteristics from the other lanthanides and actinides, especially in the trivalent oxidation state, is central to developing new separations strategies.[2−4] Soft donor ligands have recently come to the forefront of improving separation techniques[5,6] in part due to actinides showing enhanced extraction with sulfur-based agents as compared to lanthanides.[5,7] While the origin of this dichotomy is currently under investigation, current findings suggest that the higher degree of covalency in actinide−ligand bonding may play a role in this selectivity.[8−10]

Despite the redox chemistry and small molecule activation of U^{3+} leading to unprecedented reactivity,[11−14] relatively few trivalent uranium complexes have been isolated with a ligand capable of undergoing further functionalization. Additionally, few An^{3+} (An = actinide) complexes with soft donor chalcogen-based ligands comprised of sulfur, selenium, and/or tellurium have been reported. Rare examples of trivalent derivatives include the homoleptic complexes, $[U(N(\kappa^2\text{-}E,E'\text{-}(EPR)_2)_3]$ (R = Ph, ^{i}Pr; E = S,[8,15−17] Se,[15] Te[18]) and $U(SMes^*)_3$ (Mes^* = 2,4,6-^{t}Bu$_3$C$_6$H$_2$),[19] as well as heteroleptic $[Cp^*_2U(S^iPr)_2]^{1-}$,[20] $[Cp^*_2U(dddt)]^-$ (dddt = 5,6-dihydro-1,4-dithine-2,3-dithiolate),[21] and Tp^*_2USPh.[22] Across the actinide series, $[Pu(Se_2PPh_2)_4]^-$ has recently been reported,[10] along with americium and curium complexes of bis(2,4,4-trimethylpentyl)-dithiophosphinic acid.[23] While these represent important preliminary findings, further study on actinide−ligand bonding, especially in the +3 oxidation state, with soft donor atoms is justified.

Recently, we reported the synthesis, spectroscopic, and structural characterization of Tp^*_2USPh, a rare example of a uranium(III) phenylchalcogenide complex.[22] Given the growing interest in understanding trivalent uranium−chalcogen interactions and the lack of a self-contained chalcogenide series in this oxidation state, we targeted the synthesis and characterization of the rest of the U(III) phenylchalcogenide series, Tp^*_2UEPh (E = O, Se, Te). This family was prepared in high yields, and the identities of the compounds were verified by ^1H NMR spectroscopy, infrared spectroscopy, and in the case of Tp^*_2UTePh, X-ray crystallography. The bonding and electronic properties of this series were also explored using electronic absorption spectroscopy and computational methods to help evaluate the degree of covalency, if any, in the U(III)−E bond. Subsequent reactivity of the Tp^*_2UEPh series toward CS_2 insertion is also discussed.

Received: August 28, 2014
Published: November 21, 2014

dx.doi.org/10.1021/ic5020658 | Inorg. Chem. 2014, 53, 12977−12985

EXPERIMENTAL SECTION

General Considerations. All air- and moisture-sensitive manipulations were performed using standard Schlenk techniques or an MBraun inert atmosphere drybox with an atmosphere of purified nitrogen. The MBraun drybox was equipped with a coldwell designed for freezing samples in liquid nitrogen as well as two −35 °C freezers for cooling samples and crystallizations. Solvents for sensitive manipulations were dried and deoxygenated using literature procedures with a Seca solvent purification system.[24] Benzene-d_6 was purchased from Cambridge Isotope Laboratories, dried with molecular sieves and sodium, and degassed by three freeze−pump−thaw cycles. Depleted uranium was purchased from Manufacturing Science in Oak Ridge, TN. NOTE: Depleted uranium (primarily isotope ^{238}U) is a weak α-emitter with a half-life of 4.47×10^9 years. All handling should be performed in fume hoods, using Schlenk lines, or in an inert-atmosphere drybox with proper PPE and monitoring devices. Diphenyl disulfide, diphenyl diselenide, diphenyl ditelluride, and phenol were purchased from Sigma-Aldrich and dried under a vacuum prior to use. Anhydrous carbon disulfide was purchased from Sigma-Aldrich, dried over CaH_2, and distilled prior to use. Elemental analyses were performed by Midwest Microlabs LLC in Indianapolis, IN, and Atlantic Microlabs Inc. in Norcross, GA. Tp*$_2$UCH$_2$Ph[25] was synthesized according to a literature procedure.

^{1}H NMR spectra were recorded on a Varian Inova 300 spectrometer operating at a frequency of 299.992 MHz. All chemical shifts were reported relative to the peak for $SiMe_4$ using ^{1}H (residual) chemical shifts of the solvent as a secondary standard. The spectra for paramagnetic molecules were obtained using an acquisition time of 0.5 s; thus the peak widths reported have an error of ±2 Hz. For paramagnetic molecules, the ^{1}H NMR data are reported with the chemical shift, followed by the peak width at half height in Hertz, the integration value, and where possible, the peak assignment. ^{11}B NMR spectra were recorded on a Varian Mercury-300 spectrometer operating at a frequency of 96.24 MHz. All chemical shifts were reported relative to the peak for $BF_3{\cdot}Et_2O$ (0 ppm). Solid state infrared spectra were recorded using a PerkinElmer FT-IR Spectrum RX I spectrometer. Samples were made by crushing the solids, mixing with dry KBr, and pressing into a pellet. Electronic absorption measurements were recorded at 294 K in THF in a sealed 1 cm quartz cuvette with a Jasco V-670 spectrophotometer.

Single crystals of Tp*$_2$UTePh (**4**) for X-ray diffraction were coated with polybutenes oil in a glovebox and quickly transferred to the goniometer head of a Nonius KappaCCD image plate diffractometer equipped with a graphite crystal, incident beam monochromator. Preliminary examination and data collection were performed with Mo Kα radiation (λ = 0.71073 Å). Single crystals of Tp*$_2$U(κ^2-S$_2$CSPh) (**5**) for X-ray diffraction were coated with polybutenes oil in a glovebox and quickly transferred to the goniometer head of a Rigaku Rapid II image plate diffractometer equipped with a MicroMax002+ high intensity copper X-ray source with confocal optics. Preliminary examination and data collection were performed with Cu Kα radiation (λ = 1.54184 Å). Cell constants for data collection were obtained from least-squares refinement. The space groups were identified using the program XPREP.[26] The structures were solved using the structure solution program PATTY in DIRDIFF99.[27] Refinement was performed on a LINUX PC using SHELX-97.[26] The data were collected at a temperature of 150(1) K.

Magnetic susceptibility (dc) data for **4** were collected with a Quantum Design MPMS-XL SQUID magnetometer in the temperature range 4−300 K at an applied field of 1000 Oe. Powdered microcrystalline samples were loaded into gelatin capsules in the glovebox, inserted into a straw and transported to the SQUID magnetometer under dinitrogen. The absence of significant ferromagnetic impurities was confirmed for each sample by observing a linear relationship between magnetization and applied field (0.1−5 T) at 125 K. Susceptibility data reproducibility were probed via spot checks performed on multiple samples, including separate batches: the air-sensitivity of the samples results in some variation of the room temperature μ_{eff} values but the qualitative temperature dependence of the data are reproducible. Data were corrected for the magnetization of the sample holder by subtracting the susceptibility of an empty container and for diamagnetic contributions of the sample by using Pascal's constants.

Computational Details. The electronic structures of complexes **1**−**4** were examined using the Gaussian09 suite of software[28] at the B3LYP[29] (Becke-3[30] exchange and Lee−Yang−Parr[31] correlation functional) level. Full geometry optimizations were performed, and stationary points were determined to be global minima using analytical frequency calculations with the Stuttgart/Dresden triple-ζ quality basis set[32] and the corresponding effective core potential (ECP). For uranium, the most diffuse s, p, d, and f functions were removed, leaving a basis set of 7s/6p/5d/3f. For sulfur, selenium, and tellurium the LANL-DZ2P basis set was employed.[33] The Pople double-ζ quality basis set, 6-31G(d,p),[34,35] was used for all remaining atoms. Complex **1** was found to be difficult to converge at the global minimum so we report the geometry with one imaginary frequency.

Preparation of Tp$_2$U(OPh) (**1**).* A 20 mL scintillation vial was charged with Tp*$_2$UCH$_2$Ph (0.100 g, 0.108 mmol) and approximately 3 mL of THF. This dark green solution was cooled to −35 °C. In a separate vial, an equivalent of phenol (0.011 g, 0.117 mmol) was dissolved in approximately 3 mL of diethyl ether. The clear phenol solution was added to the uranium solution, resulting in an instantaneous color change to purple. After 5 min of stirring, solvents were removed under reduced pressure. The remaining dark residue was washed with cold ether/pentane (1:20), allowing isolation of Tp*$_2$U(OPh) as a purple solid. Yield = 0.085 g (0.092 mmol, 85%). Analysis for $C_{36}H_{49}N_{12}B_2UO_1$: Calcd C, 46.72; H, 5.34; N, 18.16. Found C, 46.66; H, 5.42; N, 17.98. ^{1}H NMR (C_6D_6, 25 °C): δ = −12.84 (33.4, 18H, Tp*-CH_3), −0.83 (5.13, 18H, Tp*-CH_3), 4.85 (141.2, 2H, B-*H*) 7.14 (7.1, 6H, Tp*-C*H*), 18.35 (32.9, 1H, *p*-C*H*), 21.26 (43.0, 2H, *m*-C*H*), 42.57 (79.3, 2H, *o*-C*H*). IR: 2538, 2551 cm^{-1} (B−H). ^{11}B NMR (C_6D_6, 25 °C): δ = −1.2 (H-*B*, Tp*).

General Preparation of Tp*$_2$UEPh (E = S, Se, Te). A 20 mL scintillation vial was charged with Tp*$_2$UCH$_2$Ph (0.100 g, 0.108 mmol) and approximately 5 mL of THF. In a separate vial, one-half equivalent of PhEEPh [E = S (0.011 g, 0.054 mmol); Se (0.017 g, 0.054 mmol); Te (0.022 g, 0.054 mmol)] was dissolved in diethyl ether and added dropwise to the prepared solution of Tp*$_2$UCH$_2$Ph, causing immediate darkening. After 5 min, solvents were removed *in vacuo*.

Tp$_2$USPh (**2**).* The product was washed with pentane to remove bibenzyl, leaving dark blue powder (0.094 g, 0.100 mmol, 96%). Compound **2** was characterized by ^{1}H NMR and IR spectroscopies against previously published data.[22] ^{11}B NMR (C_6D_6, 25 °C): δ = 0.1 (H-*B*, Tp*).

Tp$_2$USePh (**3**).* The blue-green residue left in the vial was washed with cold pentane producing a green solid (0.098 g, 0.100 mmol, 96%). Analysis for $C_{36}H_{49}N_{12}B_2Se_1U_1$. Calcd C, 43.74; H, 5.00; N, 17.00. Found C, 43.77; H, 5.05, N, 17.01. ^{1}H NMR (C_6D_6, 25 °C): δ = −11.34 (38, 18H, Tp*-CH_3), −0.68 (20, 18H, Tp*-CH_3), 5.43 (802, 2H, B-*H*), 7.36 (20, 6H, Tp*-C*H*), 11.00 (7, 1H, *p*-C*H*), 12.97 (24, 2H, *m*-C*H*), 19.38 (33, 2H, *o*-C*H*). IR: 2523, 2549 cm^{-1} (B-*H*). ^{11}B NMR (C_6D_6, 25 °C): δ = −0.6 (H-*B*, Tp*).

Tp$_2$UTePh (**4**).* The remaining blue solid was recrystallized from a pentane and THF mixture (2:1) resulting in the isolation of a blue solid (0.076 g, 0.074 mmol, 69%). Analysis for $C_{36}H_{49}N_{12}B_2Te_1U_1$. Calcd C, 41.69; H, 4.76; N, 16.21. Found C, 41.48; H, 4.87; N, 15.96. ^{1}H NMR (C_6D_6, 25 °C): δ = −10.89 (22, 18H, Tp*-CH_3), −0.50 (8, 18H, Tp*-CH_3), 6.41 (447, 2H, B-*H*), 7.08 (8, 6H, Tp*-C*H*), 10.44 (34, 1H, *p*-C*H*), 12.37 (54, 2H, *m*-C*H*), 18.48 (85, 2H, *o*-C*H*). IR: 2521, 2552 cm^{-1} (B-*H*). ^{11}B NMR (C_6D_6, 25 °C): δ = −0.7 (H-*B*, Tp*).

Equilibrium Experiments for the Generation of Tp*$_2$U(κ^2-S$_2$CEPh) (5−7). A J. Young NMR tube was charged with Tp*$_2$UEPh (E = S: 0.020 g (0.021 mmol); Se: 0.020 g (0.020 mmol); E = Te: 0.020 g (0.019 mmol)) and 1.0 mL of benzene-d_6, producing a dark blue solution. The appropriate amount (S, Se = 0.5, 1.0, 1.5, 2.0 equiv; Te: 2.5, 5.0, 10.0 equiv) of a CS_2 standard solution (1.65 M in benzene-d_6) was added to the tube via microsyringe, resulting in an

dx.doi.org/10.1021/ic5020658 | Inorg. Chem. 2014, 53, 12977−12985

instantaneous color change to green. After being stirred for 10 min, the equilibrium mixture was monitored by ^{1}H NMR spectroscopy, and conversions were determined by integration versus starting material. Because of the reversibility of the insertion reaction, the products, Tp*$_2$US$_2$CEPh, could not be isolated in the solid state, precluding yield determination or elemental analysis.

Tp$_2$U(κ^2-S$_2$CSPh) (**5**).* ^{1}H NMR (C_6D_6, 25 °C): −21.76 (56, 6H, Tp*-CH_3), −11.72 (30, 6H, Tp*-CH_3), −0.83 (21, 6H, Tp*-CH_3), 1.17 (21, 6H, Tp*- CH_3), 2.18 (20, 6H, Tp*-CH_3), 3.16 (42, 6H, Tp*-CH_3), 4.02 (22, 2H, Tp*-C*H*), 6.32 (187, 2H, B-*H*), 6.92 (18, 2H, Tp*-C*H*), 7.82 (t, *J* = 7 Hz, 2H, *m*-C*H*), 8.31 (t, *J* = 7 Hz, 1H, *p*-C*H*), 10.30 (d, *J* = 7 Hz, 2H, *o*-C*H*), 11.69 (35, 2H, Tp*-C*H*). IR: 688 (C−S−C$_{asym}$), 645 (C−S−C$_{symm}$), 2522, 2548 cm^{-1} (B-*H*).

Tp$_2$U(κ^2-S$_2$CSePh) (**6**).* ^{1}H NMR (C_6D_6, 25 °C): δ = −21.37 (46, 6H, Tp*-CH_3), −11.69 (28, 6H, Tp*-CH_3), −0.84 (23, 6H, Tp*-CH_3), 1.24 (18, 6H, Tp*-CH_3), 1.79 (29, 6H, Tp*-CH_3), 3.17 (44, 6H, Tp*-CH_3), 4.18 (23, 2H, Tp*-C*H*), 6.27 (407, 2H, B-*H*), 6.83 (22, 2H, Tp*-C*H*), 7.84 (t, *J* = 6 Hz, 2H, *m*-C*H*), 8.32 (t, *J* = 8 Hz, 1H, *p*-C*H*), 9.49 (d, *J* = 8 Hz, 2H, *o*-C*H*), 11.75 (45, 2H, Tp*-C*H*). IR: 692 (C−S−C$_{asym}$), 645 (C−S−C$_{symm}$), 2520, 2552 cm^{-1} (B-*H*).

Tp$_2$U(κ^2-S$_2$CTePh) (**7**).* ^{1}H NMR (C_6D_6, 25 °C): δ = −20.74 (78, 6H, Tp*-CH_3), −11.37 (35, 6H, Tp*-CH_3), −0.83 (36, 6H, Tp*-CH_3), 1.25 (35, 6H, Tp*-CH_3), 1.44 (40, 6H, Tp*-CH_3), 3.07 (68, 6H, Tp*-CH_3), 4.23 (38, 2H, Tp*-C*H*), 6.22 (202, 2H, B-*H*), 6.78 (32, 2H, Tp*-C*H*), 7.79 (t, *J* = 8 Hz, 2H, *m*-C*H*), 8.24 (t, *J* = 6, 1H, *p*-C*H*), 9.59 (d, *J* = 6 Hz, 2H, *o*-C*H*), 11.63 (59, 2H, Tp*-C*H*). IR: 692 (C−S−C$_{asym}$), 646 (C−S−C$_{symm}$), 2523, 2548 cm^{-1} (B-*H*).

Crystallization of Tp$_2$U(κ^2-S$_2$CSPh) (**5**).* A 20 mL scintillation vial was charged with **2** (100 mg, 0.110 mmol) and approximately 1 mL of a THF/toluene mixture (1:1) and cooled to −35 °C. In a separate vial, CS_2 (6.7 μL, 0.110 mmol) was dissolved in approximately 2 mL of pentane and cooled to −35 °C. The solution of CS_2 was slowly layered on top of the THF solution of complex **2** and stored at −35 °C overnight. After 12 hours, bright green crystals collected on the bottom of the vial.

RESULTS AND DISCUSSION

Synthesis and Characterization of Tp*$_2$UEPh Complexes. In order to explore the bonding and reactivity in the series of trivalent uranium phenylchalcogenide complexes, Tp*$_2$UEPh (E = O, S, Se, Ph), synthesis of each compound was initially targeted. The oxygen congener, Tp*$_2$UOPh (**1**), was generated by treating a green solution of Tp*$_2$UCH$_2$Ph with an equivalent of phenol, which resulted in a purple powder after workup (eq 1). Examination of the organics from a sealed

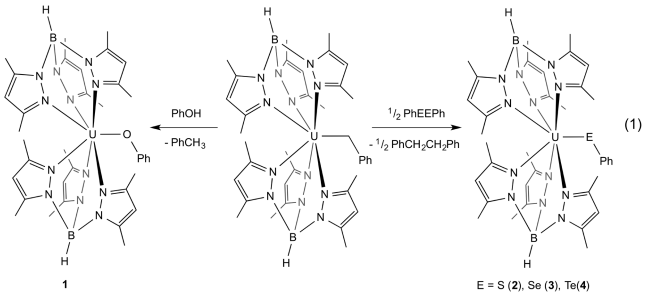

tube experiment by ^{1}H NMR spectroscopy showed the formation of toluene, indicating successful protonation of the U−C bond. The rest of the family of phenylchalcogenides was accessible by adding one-half equivalent of PhEEPh (E = S, Se, or Te) to THF solutions of Tp*$_2$UCH$_2$Ph, causing immediate color changes to blue (eq 1). In each case, rapid formation of the phenylchalcogenide product, Tp*$_2$UEPh (E = S (**2**), Se (**3**), Te (**4**)) was observed along with one-half equivalent of bibenzyl as identified by ^{1}H NMR spectroscopy. Performing the synthesis of **2** in the presence of 1,4-cyclohexadiene showed formation of toluene rather than bibenzyl, supporting the presence of benzyl radicals in solution during the preparation of **2**−**4**.

Analysis of complexes **1**−**4** by ^{1}H NMR spectroscopy showed analogous symmetric spectra with seven paramagnetically broadened and shifted resonances (Figure 1). The

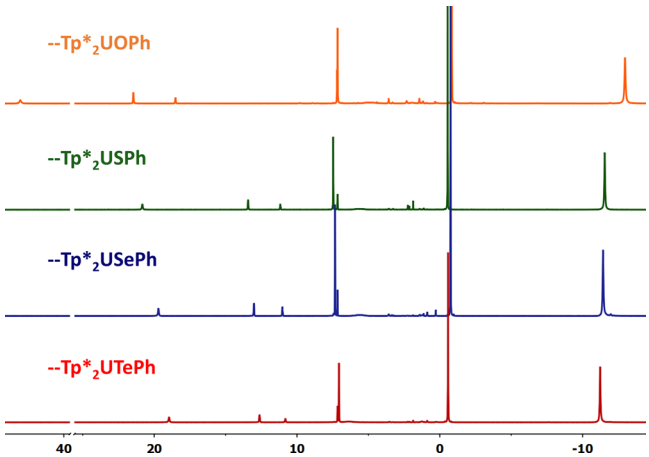

Figure 1. Comparison of ^{1}H NMR spectroscopic data for Tp*$_2$UEPh [E = O (**1**), S (**2**), Se (**3**), Te (**4**)] measured in benzene-d_6 at 25 °C.

resonances for the Tp* *endo* methyl groups range from −10 to −13 ppm, while those for the equivalent *exo* Tp* protons appear from 0 to −1 ppm. The equivalent pyrazole protons of the Tp* ligand all appear around 7 ppm, while the broad resonance of the B−H is evident from 4 to 7 ppm for **1**−**4**. For **1**, signals at 18.35, 21.26, and 42.57 ppm are assigned as the protons of the phenyl group, reflective of free rotation in solution and similar to C_2 symmetric Tp*$_2$UOMes (Mes = 2,4,6-trimethylphenyl).[36] For compounds **2**−**4**, these equivalent phenyl resonances are noted by an upfield shift relative to **1**, ranging from 10 to 21 ppm. The ^{1}H NMR spectrum for **2** matches that previously reported, which was originally synthesized by the addition of thiophenol to Tp*$_2$UCH$_2$Ph.[22]

The ^{1}H NMR spectral data for **1**−**4** show that the resonances shift toward the diamagnetic region as the radius of the chalcogenide bonded to uranium increases. For example, in Tp*$_2$UOPh (**1**), the *endo*-Tp* methyl appears at −12.97 ppm, and shifts downfield (S = −11.55; Se = −11.34, Te = −10.89 ppm) as Group 16 is descended. Likewise, the corresponding trend is noted for the -EPh protons for **1**−**4**, which shift upfield as the distance between the paramagnetic uranium center and phenyl protons increases on account of the larger chalcogen. It should be noted that this shifting is not as extreme between sulfide, selenide and telluride species as it is in the case of the oxygen analogue, **1**. This has also been noted in the series of complexes, Cp*$_2$U(EPh)$_2$ (E = S,[37] Se,[38] Te[39]), where the Cp* and -EPh resonances shift according to the same trend as for Tp*$_2$UEPh.

Compound **4** was also characterized by X-ray crystallography, as little structural data exists for uranium(III)-telluride interactions. Blue, block-shaped crystals grown from a concentrated solution of toluene and diethyl ether (1:2) over 48 h at −35 °C were analyzed, and refinement of the data revealed a seven-coordinate uranium center in a capped octahedral geometry (Figure 2, structural parameters in Table 1). One triangular face of the octahedron is formed by N21,

dx.doi.org/10.1021/ic5020658 | Inorg. Chem. 2014, 53, 12977−12985

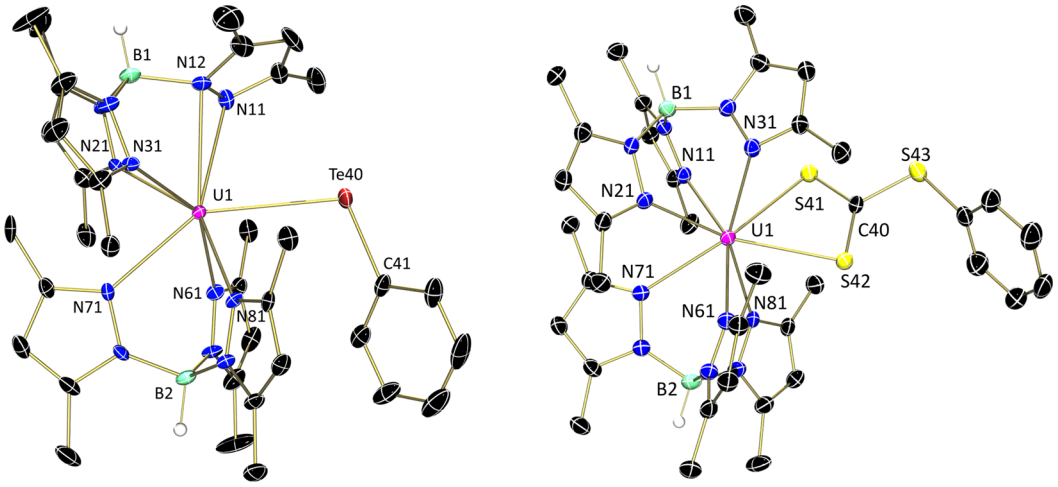

Figure 2. Molecular structure of **4** (left) and **5** (right) shown with 30% probability ellipsoids. Selected hydrogen atoms and cocrystallized solvent molecules have been omitted for clarity.

Table 1. Structural Parameters of 4 and 5

bond	4	5	bond	4	5
U1−N11	2.844(7) Å	2.555(4) Å	U1−S41		2.9643(13) Å
U1−N12	2.829(6) Å		U1−S42		2.9756(13) Å
U1−N21	2.547(7) Å	2.598(4) Å	S41−C40		1.698(5) Å
U1−N31	2.577(6) Å	2.716(4) Å	S42−C40		1.678(5) Å
U1−N61	2.483(7) Å	2.579(4) Å	S41−C40−S42		123.9(3)°
U1−N71	2.660(6) Å	2.678(5) Å	S41−U1−S42		60.19(3)°
U1−N81	2.541(6) Å	2.707(4) Å			
U1−Te40	3.2392(6) Å				
U1−Te40−C41	106.0(2)°				

N31, and N71, while the other is composed of N61, N81, and the midpoint of N11−N12, and is capped by the tellurium atom. The U−N distances for the Tp* ligands, ranging from 2.483(7) to 2.844(7) Å, are consistent with those observed for bis-Tp* complexes and Tp^*_2USPh (**2**).[22,25] The unusual coordination for **4**, where a single Tp* ligand is coordinated in a κ^4 fashion, has been observed previously for Tp^*_2UI.[40] The U−N distances of the η^2-pyrazole ring of Tp^*_2UI (2.807(5) and 2.833(5) Å) compare favorably with that of complex **4**, which has corresponding distances of 2.844(7) and 2.829(6) Å. The unusual κ^4-coordination of the Tp* ligand is not observed in the solution ^{1}H NMR spectrum, as all *endo*-protons of the Tp* are equivalent and chemically distinct from the *exo*-Tp* methyl groups, which are equivalent to each other.

The U−Te distance in **4** of 3.2392(6) Å is similar to that in the homoleptic uranium(III) telluride complex, $[U(N(\kappa^2\text{-}Te,Te'\text{-}(TePPh)_2)_3]$, which has distances ranging from 3.1270(7) to 3.1990(7) Å,[18] but is slightly longer than those in tetravalent $Cp^*_2U(TePh)_2$ (3.0383(6) Å),[39] $Cp^*_2U(\eta^2\text{-}TeC_6H_4)$ (2.9648(4) Å),[39] and bis-μ-telluride $[Na(DME)_3]_2[\{((^{Ad}ArO)_3N)U\}_2(\mu\text{-}Te)_2]$ (3.031(1), 3.112(1) Å).[41] As expected, this U−Te distance in **4** is also longer than that in pentavalent $Cp^*_2U(=N\text{-}2,6\text{-}{}^iPr_2\text{-}C_6H_3)(TePh)$ (3.0845(9) Å)[42] and hexavalent $[U(N{}^tBu)_2(TePh)_2({}^tBu_2bpy)]$ (3.0405(8) and 3.0335(8) Å)[43] due to the larger ionic radius of U^{3+} as compared to U^{5+} and U^{6+}. The smaller U−Te−C angle in **4** of 106.0(2)° as compared to that of the sulfur analogue, **2** (113.8(2)°), is consistent with the decreasing degree of s-hybridization moving down the chalcogen series and has been observed in lanthanide[44] and uranium[38,39,43] phenylchalcogenide families.

Previous analysis by Arnold et al. has shown that structural parameters may be used as an indicator to determine the extent of covalency in actinide-chalcogen bonding.[45] For instance, in the series Cp^*_2UOPh, $Cp^{Me4}{}_2USPh$, Cp^*_2USePh, and Cp^*_2UTePh, the short U−O distance relative to the other compounds was determined to be a result of steric crowding and an increased ionic contribution to bonding from a U^+—O^- resonance form rather than of a O→ U π donation. While the crystallographic data for the Tp* series is not complete, comparison of Tp^*_2UOMes,[36] Tp^*_2USPh, and Tp^*_2UTePh is possible. As in the uranium(IV) series, the data for these trivalent derivatives show the same trends, with an unusually short U−O distance as compared to the sum of the U and O covalent radii as well as the largest U−E−C angle of the series (Table 2). This short U−O bond distance indicates a large degree of ionic character in this trivalent series.

Table 2. Structural Parameters for Tp^*_2UOMes,[36] Tp^*_2USPh, and Tp^*_2UTePh[a]

compound	avg U−E	avg U−E−C	E ionic radius	effective U radius
Tp^*_2UOMes	2.159(10)	168.2(10)	1.35	0.81
Tp^*_2USPh	2.857(15)	113.8(2)	1.84	1.02
Tp^*_2UTePh	3.2392(6)	106.0(2)	2.21	1.03

[a]The ionic radius of the chalcogenide as reported in ref 45 and the calculated effective U radius are also shown.

dx.doi.org/10.1021/ic5020658 | *Inorg. Chem.* 2014, 53, 12977−12985

Electronic Absorption Spectroscopy. The optical properties of complexes **1**−**4** were examined by electronic absorption spectroscopy. Data for the series were recorded in THF over the range of 400−2100 nm, (Figure 3) and showed analogous low-to-mid intensity absorption bands distributed throughout the UV and visible regions. Complexes **1** and **2** have sharp, color producing d-f charge-transfer bands at 578 nm (**1**: ε = 767 $M^{-1}cm^{-1}$; **2**: ε = 788 $M^{-1}cm^{-1}$), whereas these appear at 575 nm for **3** (ε = 771 $M^{-1}cm^{-1}$) and **4** (ε = 836 $M^{-1}cm^{-1}$).[46] These bands in the visible region, as well as those present throughout the near-infrared region of the spectra, show weak, ill-defined parity forbidden f−f transitions for **1**−**4**, confirming the +3 oxidation state of uranium.[46,47] Prominent features in the near-infrared regions include the sharp bands between 1150 and 1350 nm for **1**−**4**; however, the bands for **1** differ from those for **2**−**4**. For **1**, this band is visible at 1189 nm (ε = 246 M^{-1} cm^{-1}) and appears to red shift as group 16 is descended. For **2**, this band is evident at 1244 nm (ε = 169 M^{-1} cm^{-1}) and shifts farther to 1251 nm for **3** (ε = 156 M^{-1} cm^{-1}) and **4** (ε = 170 M^{-1} cm^{-1}). An additional feature located at 2017 nm (ε = 116 M^{-1} cm^{-1}) is observed in the spectrum of Tp*$_2$UOPh but is not visible within the range of the experiment for the rest of the series. Changes in features in the f−f spectral region for a chalcogen series of uranium complexes has been observed for the pentavalent family, Cp*$_2$U(=N-2,6-^{i}Pr$_2$-C$_6$H$_3$)(EPh) (E = O, S, Se, Te), reported by Kiplinger and co-workers.[48,49] Similar to **1**−**4**, this family shows a significant change in optical properties between the aryloxide and thiophenoxide species (E = O → S), while the heavier, "softer" organochalcogenide species (E = S, Se, Te) have largely the same transitions. The authors attribute the difference in spectra within the Cp*$_2$U(=N-2,6-^{i}Pr$_2$-C$_6$H$_3$)-(EPh) family to variation in f-orbital involvement of the aryloxide versus the arylsulfide, selenide, or telluride ligands, prompting further exploration of **1**−**4** through computational experiments.

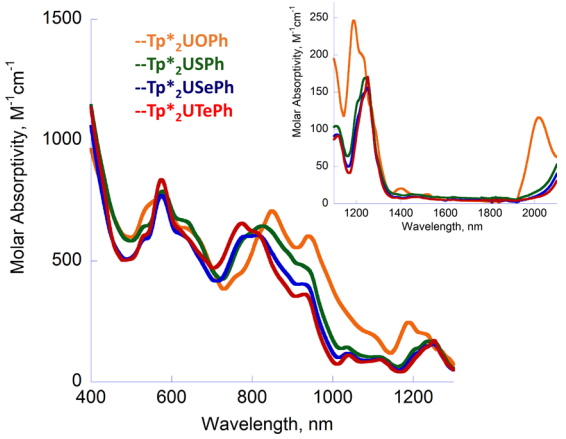

Figure 3. Electronic absorption spectra of Tp*$_2$UOPh (**1**, orange), Tp*$_2$USPh (**2**, green), Tp*$_2$USePh (**3**, blue), and Tp*$_2$UTePh (**4**, red) in THF at ambient temperature. Inset shows the near-infrared region of the spectra. Solvent overtones between 1670 and 1760 nm have been removed for clarity.

Magnetism. The lack of magnetic data for trivalent uranium compounds containing U−Te bonds prompted exploration of **4** by SQUID magnetometry (Figure 4). The room temperature moment of 3.58 μ_B (295 K) for **4** is just slightly below what would be expected for a free U(III) ion ($^4I_{9/2}$, 3.62 μ_B).[11] This moment decreases gradually to 2.86 μ_B at 7 K. Only below this temperature does a more significant drop occur, to 2.77 μ_B at 4 K. The decrease in the effective magnetic moment as temperature decreases is less drastic than what is observed for uranium(IV) compounds with similar ligand sets but is more like trivalent Tp*$_2$UI.[50] While Tp*$_2$UI has μ_{eff} = 3.01 μ_B at 300 K, **4** shows higher room and low temperature moments. Interestingly, both Tp*$_2$UI and the recently reported [Tp*$_2$U-(bpy)][I][51] behave as single-molecule magnets. Given the structural similarity of **4** to these species, combined with the slow relaxation of magnetization typically observed in other U(III) complexes,[52,53] **4** may also be a candidate to show single-molecule magnetic properties.

Computation. The electronic structures of complexes **1**−**4** were examined by density functional theory (DFT) at the B3LYP[29] level of theory. Complexes **2** and **4** were optimized from their coordinates generated from X-ray crystallographic analyses. Upon successful optimization of **2**, the sulfur atom was replaced with oxygen or selenium and reoptimized to afford **1** and **3**, respectively. The calculated uranium−sulfur and uranium−tellurium bond distances of 2.832 (**2**) and 3.233 Å (**4**), respectively, are nearly identical to the experimentally determined lengths of 2.8573(15) and 3.2392(6) Å. Additionally, the calculated U−Te−C angle of 106.88° is close to the

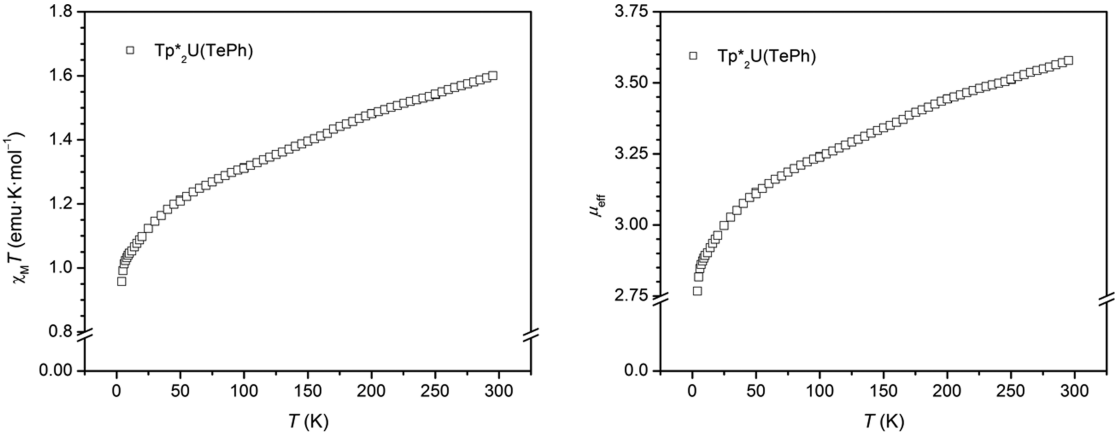

Figure 4. Susceptibility (left) and effective magnetic moment (right) versus temperature for Tp*$_2$UTePh (**4**). Susceptibility data were collected at a 1000 Oe measuring field.

dx.doi.org/10.1021/ic5020658 | Inorg. Chem. 2014, 53, 12977−12985

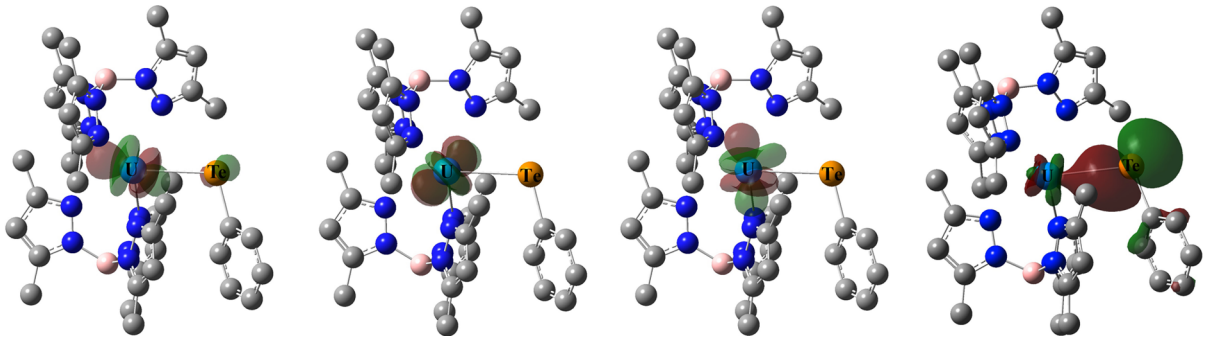

Figure 5. Visualization of orbitals for Tp*$_2$UTePh (**4**). HOMO (left), HOMO-1 (left middle), and HOMO-2 (right middle) depict the uranium based f-orbitals that each house one of the three unpaired electrons for the U(III), 5f^3 ion. HOMO-3 (right) shows the U−Te σ-bond in complex **4**.

experimental bond angle of 106.0(2)° for **4**. The uranium−oxygen bond distance for **1** was calculated to be 2.199 Å and is similar to those observed for the terminal aryloxide ligands in $[U(O\text{-}2,6\text{-}^iPr_2C_6H_3)_3]_2$ (2.214(7) Å)[54] and on the order of that in Tp*$_2$UOMes (2.159(10) Å).[36] No terminal organoselenide complexes of U(III) exist for comparison with **3**, but the theoretical uranium−selenium bond distance calculated for **3** of 2.997 Å is slightly shorter than that of 3.0869(4) Å, which was observed for trivalent $[U(N(\kappa^2\text{-}Se,Se'\text{-}(SePPh)_2)_3]$. The calculated distance for **3** is also longer than that for uranium−phenylselenide bonds in tetravalent Cp*$_2$U(SePh)$_2$ (2.8011(7), 2.7997(7) Å), which is expected as the uranium(III) ionic radius is ∼0.1 Å longer than the radius for uranium(IV).[55]

The electronic structures of complexes **1**−**4** were established by examining the Mulliken spin densities for uranium. This parameter is a useful metric for paramagnetic molecules as it shows the amount of electron density being gained or donated from bonded atoms and is, in general, more independent from functional and basis set than Mulliken population analysis.[56,57] Analysis shows the family of complexes **1**−**4** consist of U(III), 5f^3 centers, with respective Mulliken spin densities of 3.005, 3.019, 3.022, and 3.027 (B3LYP). To reiterate the functional independence, the Mulliken spin densities for complexes **2** and **4** were calculated at the B3PW91 level of theory to be 3.037 and 3.046 and using PBE to be 3.006 and 3.011. The three unpaired electrons are contained in the HOMO, HOMO-1, and HOMO-2, which are mainly uranium f orbital in character (Figure 5). The spin density numbers do not deviate significantly from their expected value of 3.000 for three unpaired electrons, suggesting the U−E bond in this family is primarily ionic, with only small covalent character (Table 3). This is highlighted for compound **4** in Figure 5, which shows the uranium−tellurium bonding (HOMO-3) orbital. Here, the U−Te has a significant σ-bond with no π interaction present. Analysis of the composition of the U−Te bond shows less than 5% of 5f orbital contribution, with a 71% contribution from the Te 5p orbital. The spin density values calculated for **1**−**4** deviate from that of the U(III) center in Cp*$_2$[^{i}PrNC(Me)N^{i}Pr]U (3.079), as well as its transuranic analogues, Cp*$_2$[^{i}PrNC(Me)N^{i}Pr]An (An = Np - Am), implying the amidinate series better supports covalent bonding character with uranium.[58] The corresponding spin densities of the chalcogenides in **1**−**4** are also small; thus minimal E → U donation is observed. Therefore, the uranium−chalcogenide bond in complexes **1**−**4** can best be described as primarily ionic with a small covalent contribution.

Table 3. Mulliken Spin Densities for Complexes 1−4 Calculated at the B3LYP Level of Theory

	Mulliken spin densities		
complex	uranium(III)	*E*	Σ N (coordinated to U)
1, E = O	3.005	−0.016	−0.059
2, E = S	3.019	−0.018	−0.057
3, E = Se	3.022	−0.020	−0.057
4, E = Te	3.027	−0.024	−0.058

The computational results for **1**−**4** are consistent with those reported for the model compound, USR′(SR)$_2$ (R = 2-^{t}BuC$_6$H$_4$; R′ = C$_6$H$_5$), previously calculated for trivalent U(SMes*)$_3$. This study shows the U(III)-S bonds are ionic and strongly polarized at the sulfur.[19] However, several examples for trivalent uranium have been demonstrated to contain a small covalent component in the uranium-chalcogen bond. The trivalent anion, [Cp*$_2$U(dddt)]$^-$, was established by structural and computational analyses to possess some covalent character in the U−S bonds.[21] Similarly, results from studying the uranium(III) series, $[U(N(\kappa^2\text{-}E,E'\text{-}(EPR)_2)_3]$ (R = Ph, ^{i}Pr; E = S,[8,15−17] Se,[15] Te[18]), found a covalent contribution for the U−E bonds but also noted a slight increase in the degree of covalency as the chalcogen donor group is descended.[17] This trend can also be observed in **1**−**4** with increasing deviation from the expected spin density with concomitant increase in spin density on E and constant spin density on all nitrogen atoms. This indicates the change in spin density on the uranium is due primarily to the chalcogenide and parallels those results of previous studies in which covalent bonding increases going down the chalcogen series.[16,17] The bis(Tp*) system seems to have less covalency, which may be attributed to the fact that previous homoleptic complexes only have bonds that are uranium-chalcogenide in nature.

Reactivity of Tp*$_2$UEPh with CS$_2$. The reactivity of **2**−**4** toward carbon disulfide was explored. Layering a cold, dark blue THF solution (−35 °C) of Tp*$_2$USPh with a pentane solution of CS$_2$ of the same temperature and cooling for 12 h resulted in the deposition of large, green needles of the trithiocarbonate product, Tp*$_2$U(κ^2-S$_2$CSPh) (**5**), arising from CS$_2$ insertion into the U−S bond (eq 2). Likewise exposure of either **3** or **4** to CS$_2$ also produced the requisite color change from blue to green as seen for **2**, indicating formation of Tp*$_2$U(κ^2-S$_2$CEPh) (E = Se (**6**), Te (**7**)), respectively (eq 2). However, workup under reduced pressure for **5**−**7** returned the deep blue color of the starting material, indicating a reversible CS$_2$ insertion process for each. Thus, complexes **5**−**7** were generated in J. Young NMR tubes and characterized by ^{1}H

dx.doi.org/10.1021/ic5020658 | Inorg. Chem. 2014, 53, 12977−12985

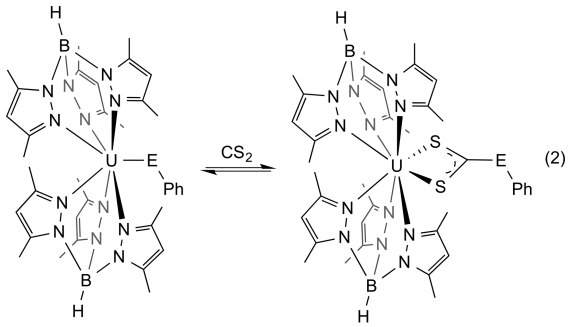

NMR spectroscopy in benzene-d_6 (Table 4) in the presence of CS_2. No reaction with carbon disulfide was noted for Tp^*_2UOPh (**1**).

Table 4. ^{1}H NMR Data for $Tp^*_2U(\kappa^2\text{-}S_2CEPh)$ (5−7) Measured in Ppm in Benzene-d_6 at 25° C

	5 (E = S)	**6** (E = Se)	**7** (E = Te)
Tp*-CH_3	−21.76, −11.72, −0.83, 1.17, 2.18, 3.16	−21.37, −11.69, −0.84, 1.24, 1.79, 3.17	−20.74, −11.34, −0.83, 1.25, 1.44, 3.07
Tp*-CH	4.02, 6.95, 11.69	4.11, 6.86, 11.75	4.23, 6.82, 11.63
B−H	6.32	6.27	6.22
m-CH	7.82	7.84	7.79
p-CH	8.31	8.32	8.24
o-CH	9.48	9.49	9.59

Analysis of **5**−**7** by ^{1}H NMR spectroscopy revealed asymmetric spectra composed of 13 paramagnetically shifted and broadened resonances analogous to $Tp^*_2U(\kappa^2\text{-}S_2CCH_2Ph)$ (Table 4).[25] The *endo*- and *exo*-methyls of the Tp* ligand are chemically inequivalent, with six resonances appearing from 3 to −22 ppm integrating to six protons each, due to the sterically bulky dithiocarboxylate ligand. The three corresponding singlets for the pyrazole protons are located in the range of 4−12 ppm, integrating to 2H. Those for phenyl protons are located from 7 to 10 ppm and are identifiable due to the presence of splitting, as these signals are now farther from the paramagnetic uranium center following CS_2 insertion.

While insertion of CS_2 into uranium−chalcogenide bonds has rarely been observed for uranium(III) species, this has been studied in tetravalent systems. For instance, Ephritikhine and co-workers showed CS_2 insertion with Cp_3US^iPr, which further reacts to form $Cp_2U(S_2CS^iPr)_2$.[59] For their related system, $Cp^*_2U(SR)_2$ (R = Me, ^{i}Pr, ^{t}Bu), CS_2 insertion generates $Cp^*_2U(SR)(S_2CSR)$,[37] from which the double insertion products, $Cp^*_2U(S_2CSMe)_2$ and $Cp^*_2U(S_2CS^tBu)_2$, can be generated with an additional equivalent of CS_2. In a similar fashion, Meyer and co-workers demonstrated reactivity of CS_2 with the sterically crowded uranium(IV) chalcogenide-bridged family $[\{((^{Ad}ArO)_3N)U\}_2(\mu\text{-}E)]$ (E = S, Se), facilitating isolation of the uranium chalcogenide mixed carbonate species $[\{((^{Ad}ArO)_3N)U\}_2(\mu\text{-}\kappa^2\text{:}\kappa^2\text{-}S_2C\text{-}E)]$.[60] In this family of molecules, no CS_2 insertion is noted at the strong U−O bonds of the supporting aryloxide ligand, which is in line with the observed lack of reactivity of **1**.

The stability of compound **5** allowed for characterization by X-ray diffraction of suitable crystals grown from layering a CS_2/pentane solution over a concentrated THF/toluene solution of **2** at −35 °C (Figure 2, Table 1). Analysis confirmed the formation of the trithiocarbonate, $Tp^*_2U(\kappa^2\text{-}S_2CSPh)$. Compound **5** has an eight coordinate uranium center similar in coordination geometry to that of $Tp^*_2U(\kappa^2\text{-}E_2CCH_2Ph)$ (E = O, S).[25] The U−N distances for the bis-Tp* framework are as expected, ranging from 2.555(4) to 2.716(4) Å.[22,25,61] The U−S distances for the trithiocarbonate ligands in **5** of 2.9643(13) and 2.9756(13) Å support the uranium(III) assignment, as these are similar to those in trivalent $Tp^*_2U(\kappa^2\text{-}S_2CCH_2Ph)$ (2.943(4), 3.016(4) Å).[25] These distances are roughly 0.1 Å longer than those in tetravalent $Cp^*_2U(S^tBu)(\kappa^2\text{-}S_2CS^tBu)$ (2.885(4), 2.821(5) Å)[37] and $[\{((^{Ad}ArO)_3N)U\}_2(\mu\text{-}\kappa^2\text{:}\kappa^2\text{-}S_2CS)]$ (2.868(2), 2.872(2) Å).[60] The C−S distances in **5** of 1.698(5) and 1.678(5) Å are within error of each other, and close to those observed for $Tp^*_2U(\kappa^2\text{-}S_2CCH_2Ph)$ (1.656(17), 1.712(16) Å)[25] and $[\{((^{Ad}ArO)_3N)U\}_2(\mu\text{-}\kappa^2\text{:}\kappa^2\text{-}S_2CS)]$ (1.707(4), 1.710(4) Å), supporting delocalization of the monoanionic charge across the bidentate trithiocarbonate ligand.

To more thoroughly explore the role of insertion equilibria in the generation of **5**−**7**, titration experiments were performed and the data is tabulated in Table S2, Supporting Information. From these experiments, equilibrium constants for compounds **5**, **6**, and **7** of 2550 ± 80, 24 ± 3, and 70 ± 2 M^{-1}, respectively, were measured. The significantly higher value for **5** as compared to **6** and **7** is consistent with higher conversions of starting material to product in the presence of excess carbon disulfide, which facilitated the isolation of X-ray quality crystals of **5**, but not for **6** or **7**. The large driving force for the formation of **5** relative to **6** and **7** can most likely be attributed to the strong C−S bond (167(2) kcal/mol)[62] that is formed by CS_2 insertion in comparison to the weaker C−Se (139(23) kcal/mol)[62] and C−Te (66 kcal/mol)[63] bonds.

CONCLUSIONS

In summary, we have synthesized and characterized a series of trivalent uranium phenylchalcogenide species, Tp^*_2UEPh (E = O (**1**), S (**2**), Se (**3**), Te (**4**)). The optical properties of these compounds have been probed using electronic absorption spectroscopy, supporting the uranium(III) oxidation states in **1**−**4**. DFT calculations show the uranium−chalcogenide bonds in compounds **1**−**4** are primarily ionic but do show the trend of increasing covalent bonding with heavier chalcogens as has been previously noted. Additionally, the U−S, U−Se, and U−Te bonds were found to undergo reversible insertion of CS_2, forming the monoanionic dithiocarboxylate ligand derivatives **5**−**7**.

The uranium(III)-chalcogen derivatives presented here are rare members of an analogous series in which the steric and electronic properties of all the other components in the system are held constant; thus a true comparison of the role of the chalcogen can be made. In analogy to the $[U(N(\kappa^2\text{-}E,E'\text{-}(EPR)_2)_3]$ series, hydrotris(3,5-dimethylpyrazolyl)borate derivatives **1**−**4** show a slight increase in covalency is noted as Group 16 is descended, with the primary contribution to bonding being ionic in character.

ASSOCIATED CONTENT

Supporting Information

^{1}H NMR spectra of **1**−**7**; electronic absorption spectra for **5**−**7**; data for equilibrium experiments; crystallographic experimental information; crystallographic information files. This material is available free of charge via the Internet at http://pubs.acs.org.

dx.doi.org/10.1021/ic5020658 | Inorg. Chem. 2014, 53, 12977−12985

AUTHOR INFORMATION

Corresponding Authors

*E-mail: sbart@purdue.edu.

*E-mail: walenskyj@missouri.edu.

Notes

The authors declare no competing financial interest.

ACKNOWLEDGMENTS

We acknowledge the National Science Foundation (CAREER grant to S.C.B., CHE-1149875; also grant to M.P.S., CHE-1058889) and the U.S. Nuclear Regulatory Commission Faculty Development Award (J.R.W.) for funding this work. We also thank Stacey Opperwall for her assistance with electronic absorption spectroscopic measurements.

REFERENCES

(1) Gras, J.-M.; Quang, R. D.; Masson, H.; Lieven, T.; Ferry, C.; Poinssot, C.; Debes, M.; Delbecq, J.-M. *J. Nucl. Mater.* **2007**, *362*, 383.

(2) Panak, P. J.; Geist, A. *Chem. Rev.* **2013**, *113*, 1199.

(3) Wang, C.-Z.; Lan, J.-H.; Wu, Q.-Y.; Zhao, Y.-L.; Wang, X.-K.; Chai, Z.-F.; Shi, W.-Q. *Dalton Trans.* **2014**, *43*, 8713.

(4) Abraham, F.; Arab-Chapelet, B.; Rivenet, M.; Tamain, C.; Grandjean, S. *Coord. Chem. Rev.* **2014**, *266*−*267*, 28.

(5) Hudson, M. J.; Harwood, L. M.; Laventine, D. M.; Lewis, F. W. *Inorg. Chem.* **2013**, *52*, 3414.

(6) Kolarik, Z. *Chem. Rev.* **2008**, *108*, 4208.

(7) Lewis, F. W.; Hudson, M. J.; Harwood, L. M. *Synlett* **2011**, *2011*, 2609.

(8) Ingram, K. I. M.; Tassell, M. J.; Gaunt, A. J.; Kaltsoyannis, N. *Inorg. Chem.* **2008**, *47*, 7824.

(9) Arnold, P. L.; Turner, Z. R.; Kaltsoyannis, N.; Pelekanaki, P.; Bellabarba, R. M.; Tooze, R. P. *Chem.—Eur. J.* **2010**, *16*, 9623.

(10) Jones, M. B.; Gaunt, A. J.; Gordon, J. C.; Kaltsoyannis, N.; Neu, M. P.; Scott, B. L. *Chem. Sci.* **2013**, *4*, 1189.

(11) Castro-Rodriguez, I.; Meyer, K. *Chem. Commun.* **2006**, 1353.

(12) Fox, A. R.; Bart, S. C.; Meyer, K.; Cummins, C. C. *Nature* **2008**, *455*, 341.

(13) Korobkov, I.; Gambarotta, S. *Prog. Inorg. Chem.* **2005**, *54*, 321.

(14) Evans, W. J.; Kozimor, S. A. *Coord. Chem. Rev.* **2006**, *250*, 911.

(15) Gaunt, A. J.; Scott, B. L.; Neu, M. P. *Chem. Commun.* **2005**, 3215.

(16) Ingram, K. I. M.; Kaltsoyannis, N.; Gaunt, A. J.; Neu, M. P. *J. Alloys Compd.* **2007**, *444*−*445*, 369.

(17) Gaunt, A. J.; Reilly, S. D.; Enriquez, A. E.; Scott, B. L.; Ibers, J. A.; Sekar, P.; Ingram, K. I. M.; Kaltsoyannis, N.; Neu, M. P. *Inorg. Chem.* **2008**, *47*, 29.

(18) Gaunt, A. J.; Scott, B. L.; Neu, M. P. *Angew. Chem., Int. Ed.* **2006**, *45*, 1638.

(19) Roger, M.; Barros, N.; Arliguie, T.; Thuery, P.; Maron, L.; Ephritikhine, M. *J. Am. Chem. Soc.* **2006**, *128*, 8790.

(20) Arliguie, T.; Lescop, C.; Ventelon, L.; Leverd, P. C.; Thuery, P.; Nierlich, M.; Ephritikhine, M. *Organometallics* **2001**, *20*, 3698.

(21) Roger, M.; Belkhiri, L.; Thuery, P.; Arliguie, T.; Fourmigue, M.; Boucekkine, A.; Ephritikhine, M. *Organometallics* **2005**, *24*, 4940.

(22) Matson, E. M.; Fanwick, P. E.; Bart, S. C. *Organometallics* **2011**, *30*, 5753.

(23) Jensen, M. P.; Bond, A. H. *J. Am. Chem. Soc.* **2002**, *124*, 9870.

(24) Pangborn, A. B.; Giardello, M. A.; Grubbs, R. H.; Rosen, R. K.; Timmers, F. J. *Organometallics* **1996**, *15*, 1518.

(25) Matson, E. M.; Forrest, W. P.; Fanwick, P. E.; Bart, S. C. *J. Am. Chem. Soc.* **2011**, *133*, 4948.

(26) Sheldrick, G. M. *Acta Crystallogr.* **2008**, *112*, A64.

(27) Beurskens, P. T.; Beurskens, G.; de Gelder, R.; Garcia-Granda, S.; Gould, R. O.; Smits, J. M. M. *DIRDIF2008 Program System*; Crystallography Laboratory, University of Nijmegen: The Netherlands, 2008.

(28) Frisch, M. J.; Trucks, G. W.; Schlegel, H. B.; Scuseria, G. E.; Robb, M. A.; Cheeseman, J. R.; Scalmani, G.; Barone, V.; Mennucci, B.; Petersson, G. A.; Nakatsuji, H.; Caricato, M.; Li, X.; Hratchian, H. P.; Izmaylov, A. F.; Bloino, J.; Zheng, G.; Sonnenberg, J. L.; Hada, M.; Ehara, M.; Toyota, K.; Fukuda, R.; Hasegawa, J.; Ishida, M.; Nakajima, T.; Honda, Y.; Kitao, O.; Nakai, H.; Vreven, T.; Montgomery Jr., J. A.; Peralta, J. E.; Ogliaro, F.; Bearpark, M. J.; Heyd, J.; Brothers, E. N.; Kudin, K. N.; Staroverov, V. N.; Kobayashi, R.; Normand, J.; Raghavachari, K.; Rendell, A. P.; Burant, J. C.; Iyengar, S. S.; Tomasi, J.; Cossi, M.; Rega, N.; Millam, N. J.; Klene, M.; Knox, J. E.; Cross, J. B.; Bakken, V.; Adamo, C.; Jaramillo, J.; Gomperts, R.; Stratmann, R. E.; Yazyev, O.; Austin, A. J.; Cammi, R.; Pomelli, C.; Ochterski, J. W.; Martin, R. L.; Morokuma, K.; Zakrzewski, V. G.; Voth, G. A.; Salvador, P.; Dannenberg, J. J.; Dapprich, S.; Daniels, A. D.; Farkas, Ö.; Foresman, J. B.; Ortiz, J. V.; Cioslowski, J.; Fox, D. J. *Gaussian 09*; Gaussian, Inc.: Wallingford, CT, USA, 2009.

(29) Stephens, P. J.; Devlin, F. J.; Chabalowski, C. F.; Frisch, M. J. *J. Chem. Phys.* **1994**, 98.

(30) Becke, A. D. *J. Chem. Phys.* **1993**, *98*, 5648.

(31) Lee, C.; Yang, W.; Parr, R. G. *Phys. Rev. B* **1988**, *37*, 785.

(32) Küchle, W.; Dolg, M.; Stoll, H.; Preuss, H. *J. Chem. Phys.* **1994**, *100*, 7535.

(33) Hay, P. J.; Wadt, W. R. *J. Chem. Phys.* **1985**, *82*, 299.

(34) Hariharan, P. C.; Pople, J. A. *Theor. Chim. Acta* **1973**, *28*, 213.

(35) Francl, M. M.; Pietro, W. J.; Hehre, W. J.; Binkley, J. S.; Gordon, M. S.; DeFrees, D. J.; Pople, J. A. *J. Chem. Phys.* **1982**, *77*, 3654.

(36) Antunes, M. A.; Domingos, A.; Cordeiro dos Santos, I.; Marques, N.; Takats, J. *Polyhedron* **2005**, *24*, 3038.

(37) Lescop, C.; Arliguie, T.; Lance, M.; Nierlich, M.; Ephritikhine, M. *J. Organomet. Chem.* **1999**, *580*, 137.

(38) Evans, W. J.; Miller, K. A.; Kozimor, S. A.; Ziller, J. W.; DiPasquale, A. G.; Rheingold, A. L. *Organometallics* **2007**, *26*, 3568.

(39) Evans, W. J.; Miller, K. A.; Ziller, J. W.; DiPasquale, A. G.; Heroux, K. J.; Rheingold, A. L. *Organometallics* **2007**, *26*, 4287.

(40) Sun, Y.; McDonald, R.; Takats, J.; Day, V. W.; Eberspacher, T. A. *Inorg. Chem.* **1994**, *33*, 4433.

(41) Lam, O. P.; Heinemann, F. W.; Meyer, K. *Chem. Sci.* **2011**, *2*, 1538.

(42) Graves, C. R.; Scott, B. L.; Morris, D. E.; Kiplinger, J. L. *Chem. Commun.* **2009**, 776.

(43) Spencer, L. P.; Yang, P.; Scott, B. L.; Batista, E. R.; Boncella, J. M. *Inorg. Chem.* **2009**, *48*, 2693.

(44) Evans, W. J.; Bloom, I.; Hunter, W. E.; Atwood, J. L. *Organometallics* **1985**, *4*, 112.

(45) Minasian, S. G.; Krinsky, J. L.; Arnold, J. *Chem.—Eur. J.* **2011**, *17*, 12234.

(46) Katz, J.; Morss, L. R.; Seaborg, G. T. *The Chemistry of the Actinide Elements*; Chapman Hall: New York, 1980.

(47) Nakai, H.; Hu, X.; Zakharov, L. N.; Rheingold, A. L.; Meyer, K. *Inorg. Chem.* **2004**, *43*, 855.

(48) Graves, C. R.; Kiplinger, J. L. *Chem. Commun.* **2009**, 3831.

(49) Graves, C. R.; Scott, B. L.; Morris, D. E.; Kiplinger, J. L. *J. Am. Chem. Soc.* **2007**, *129*, 11914.

(50) Coutinho, J. T.; Antunes, M. A.; Pereira, L. C. J.; Bolvin, H.; Marcalo, J.; Mazzanti, M.; Almeida, M. *Dalton Trans.* **2012**, *41*, 13568.

(51) Antunes, M. A.; Pereira, L. C. J.; Santos, I. C.; Mazzanti, M.; Marcalo, J.; Almeida, M. *Inorg. Chem.* **2011**, *50*, 9915.

(52) Rinehart, J. D.; Long, J. R. *J. Am. Chem. Soc.* **2009**, *131*, 12558.

(53) Rinehart, J. D.; Meihaus, K. R.; Long, J. R. *J. Am. Chem. Soc.* **2010**, *132*, 7572.

(54) Van der Sluys, W. G.; Burns, C. J.; Huffman, J. C.; Sattelberger, A. P. *J. Am. Chem. Soc.* **1988**, *110*, 5924.

(55) Shannon, R. D. *Acta Crystallogr.* **1976**, *A32*, 751.

(56) Fortier, S.; Walensky, J. R.; Wu, G.; Hayton, T. W. *J. Am. Chem. Soc.* **2011**, *133*, 11732.

(57) Prodan, I. D.; Scuseria, G. E.; Martin, R. L. *Phys. Rev. B* **2007**, *76*, 033101.

(58) Walensky, J. R.; Martin, R. L.; Ziller, J. W.; Evans, W. J. *Inorg. Chem.* **2010**, *49*, 10007.

(59) Leverd, P. C.; Ephritikhine, M.; Lance, M.; Vigner, J.; Nierlich, M. *J. Organomet. Chem.* **1996**, *507*, 229.
(60) Lam, O. P.; Franke, S. M.; Heinemann, F. W.; Meyer, K. *J. Am. Chem. Soc.* **2012**, *134*, 16877.
(61) Matson, E. M.; Forrest, W. P.; Fanwick, P. E.; Bart, S. C. *Organometallics* **2012**, *31*, 4467.
(62) Dean, J. A. *Lange's Handbook of Chemistry*, 15th ed.; McGraw Hill: New York, 1999.
(63) McAllister, T. *J. Cryst. Growth* **1989**, *96*, 552.